The International Journal of Advanced Manufacturing Technology (2024) 130:1925–1933
https://doi.org/10.1007/s00170-023-12827-7

ORIGINAL ARTICLE

Influence of pre-treatment using non-thermal atmospheric pressure plasma jet on aluminum alloy A1050 to PEEK direct joining with hot-pressing process

Kosuke Takenaka[1] · Akiya Jinda[1] · Soutaro Nakamoto[1] · Ryosuke Koyari[1] · Susumu Toko[1] · Giichiro Uchida[2] · Yuichi Setsuhara[1]

Received: 11 July 2023 / Accepted: 1 December 2023 / Published online: 15 December 2023

Abstract
Aluminum alloy A1050 to polyetheretherketone (PEEK) direct joining with hot-pressing process via pre-treatment using non-thermal atmospheric pressure plasma jet has been performed. The effect of plasma irradiation on the tensile shear strength of A1050-PEEK direct bonded specimens joined by a combination of hot-pressing process and pre-plasma treatment using non-thermal atmospheric pressure plasma jet was investigated. A1050-PEEK bonded samples with plasma-treated PEEK only showed high tensile shear stress of 13.4 MPa. This increase in tensile shear strength is attributed to the addition of oxygen functional groups on the surface of the PEEK by reactive oxygen species produced by the plasma jet.

Keywords A1050 · PEEK · Direct joining · Dissimilar materials joining · Atmospheric pressure plasma

1 Introduction

Multi-material hybrid structures are expected to achieve optimal, lightweight, and high-performance structures by taking advantages of the various properties of different materials and have attracted attention from a variety of industries such as automotive [1], aeronautics [2], implants [3, 4]. In particular, metal-polymer hybrid materials are expected to be applied to components that require weight reduction while maintaining strength because they not only improve the overall performance of the structure, but also effectively combine the advantages of both metals and polymers. Metal-polymer hybrids have great potential because they are lighter and less expensive than metallic materials and thus contribute to weight reduction of vehicle bodies and improved fuel efficiency in the automotive field [5–7]. In addition, the use of thermoplastic as the polymer material enables bonding by applying thermal energy to the metal side, resulting in which it enables joining without the use of adhesives [8, 9] or joining materials such as screws and rivets [10, 11], and also has advantages such as high connectivity and the ability to be produced on a large scale.

In modern vehicles such as hybrid and electric vehicles, aluminum alloys and aluminum alloy-polymer hybrid materials are used for structural components of the vehicle body since these materials have high strength and lightweight [5, 12–15]. When considering the use of aluminum alloys or aluminum-alloy-polymer hybrid materials, simple replacement of conventionally used steel with these materials is costly. Therefore, it is expected to be applied to plate materials used in large areas, where efficient weight reduction of the car body can be expected while maintaining rigidity and strength at a reduced cost. For these reasons, the development of direct metal-plastic bonding technology is desired for the application of dissimilar materials such as aluminum alloys and engineering plastics to automotive components.

In hot-pressing processes, the heat sources such as ultrasonic welding [16–18], induction heating [19], laser assisted heating [20–23], and friction assisted joining [24] have been used. Generally, physical bonding by mechanical interlock (anchor effect [25]) and chemical bonding by hydrogen bonding are considered direct bonding mechanisms between metals and polymers. In metal-polymer bonding using some silane coupling agents [26, 27], covalent bonds can be

✉ Kosuke Takenaka
k_takenaka@jwri.osaka-u.ac.jp

[1] Joining and Welding Research Institute, Osaka University, 11-1 Mihogaoka, Ibaraki, Osaka 567-0047, Japan

[2] Faculty of Science and Technology, Meijo University, 1-501, Shiogamaguchi, Tempaku-ku, Nagoya 468-8502, Japan

formed between metals and polymers, but the mechanism of metal-polymer direct bonding is generally considered to be hydrogen bonding by functional groups formed on the metal or polymer surface.

One of the pre-treatment methods for physical bonding of direct metal-polymer bonding is laser texturing on metal surfaces, which is expected to enhance bonding strength by creating a physical surface structure. In laser texturing, a texture is created on the metal side with a laser in advance to allow the polymer to fully penetrate into the structure, resulting in sufficiently high bond strength [28–30]. On the other hand, hydrogen bonding, considered a direct bonding mechanism by chemical bonding, is a bonding using an attractive interaction between an oxide on the surface of the metal and a polar functional group (amino group, carboxyl group, hydroxyl group, etc.) on the polymer surface. In particular, it is important to add polar functional groups to the polymer surface due to surface treatment for joining dissimilar materials because it not only increases the number of functional groups on the surface to obtain a direct bond between the metal and the polymer with high strength and high quality, but it is possible to bond by adding new polar functional groups to polymers that do not have polar functional groups in their structure.

Currently, to add functional groups to polymers, several surface treatment methods such as chemical etching using acids and alkalis [31], UV irradiation [32], corona treatment [33], and plasma treatment [34] have been performed. Among them, plasma treatment is superior in that it can efficiently modify only desired locations of polymeric materials [34].

As a pre-treatment using plasma for metal-polymer direct bonding, the surface modification using atmospheric-pressure RF plasma jet is expected as a pre-treatment before hot-pressing. The density of oxygen radicals produced by atmospheric pressure RF plasma jets is two orders of magnitude higher than that of the conventional high-voltage pulses excited atmospheric-pressure plasma jet [35, 36]. In these processes, moreover, free radical species generated by the plasma jet and the heat flux provided by the plasma (gas temperature around 150 °C) work together to generate functional groups [35]. Therefore, polar functional groups can be efficiently added to desired positions by irradiation of radicals generated by atmospheric pressure RF plasma jets. In previous study, the direct joining of SUS304 stainless steel and polycarbonate (PC), an engineering plastic with a low glass transition point, by a combination of surface treatment and heating with atmospheric pressure RF plasma jet was performed, demonstrating that it is possible to join the dissimilar materials such as metals and polymers [37]. For engineering plastics with a high glass transition (melting) point, efficient functionalization is expected because the surface reaction can be enhanced by radical irradiation and the heat flux from the plasma using non-thermal atmospheric pressure RF plasma jet.

In this paper, aluminum alloy A1050 to polyetheretherketone (PEEK) direct joining with hot-pressing process via pre-treatment using non-thermal atmospheric pressure plasma jet has been demonstrated. The effect of atmospheric pressure RF plasma jet irradiation of A1050 and PEEK surfaces on the strength of A1050-PEEK direct bonding was investigated by observing the chemical and physical state of the surfaces with/without plasma irradiation.

2 Experimental procedures

The sheet of A1050 and PEEK (Mitsubishi chemical advanced materials, Ketron 1000, melting temperature: 340 °C) were used as metal and the thermoplastic sheet test pieces. The sheet sizes were 500 mm × 15 mm × 5 mm for both A1050 and PEEK. The A1050-PEEK direct joining with hot-pressing process via pre-treatment using a radio-frequency (RF) non-thermal atmospheric pressure Ar plasma jet[36, 37] was performed.

Figure 1a shows schematic illustration of the RF non-thermal atmospheric pressure Ar plasma source. The plasma source consisted of a quartz tube with a 15-mm-wide electrode to which radio frequency power was applied and a 5-mm-wide electrode that served as the ground electrode. The power electrode was placed upstream of the quartz tube along the gas flow, and the ground electrode was placed 5 mm from the bottom edge of that electrode. A quartz tube with an outer diameter of 6 mm and an inner diameter of 4 mm was used as the discharge tube. High-frequency power with a sinusoidal frequency of 60 MHz was used as the excitation source for the atmospheric pressure plasma jet. Ar gas was supplied as the discharge gas at a gas flow rate of 3 slm [35–37].

Figure 1b, c shows the dimensions of the specimen and the configuration of A1050 and PEEK direct joining with hot-pressing process via pre-plasma treatment. As a pre-treatment for A1050 and PEEK bonded surfaces, the plasma irradiation with an atmospheric-pressure RF plasma jet was performed on both A1050 and PEEK surfaces. Within 30 min immediately after plasma irradiation, A1050 was heated to 320 °C using a heater, and then hot-pressings were used for the joining process. The A1050 and PEEK were joined so that the overlap between the two materials was 10 mm.

The tensile shear stress of specimens bonded using by the epoxy adhesive was measured as a comparison of the bond strength of specimens bonded by the direct joining with hot-pressing process via pre-plasma treatment.

Tensile shear strength tests were performed to determine the bond strength using the tensile tester (Autograph

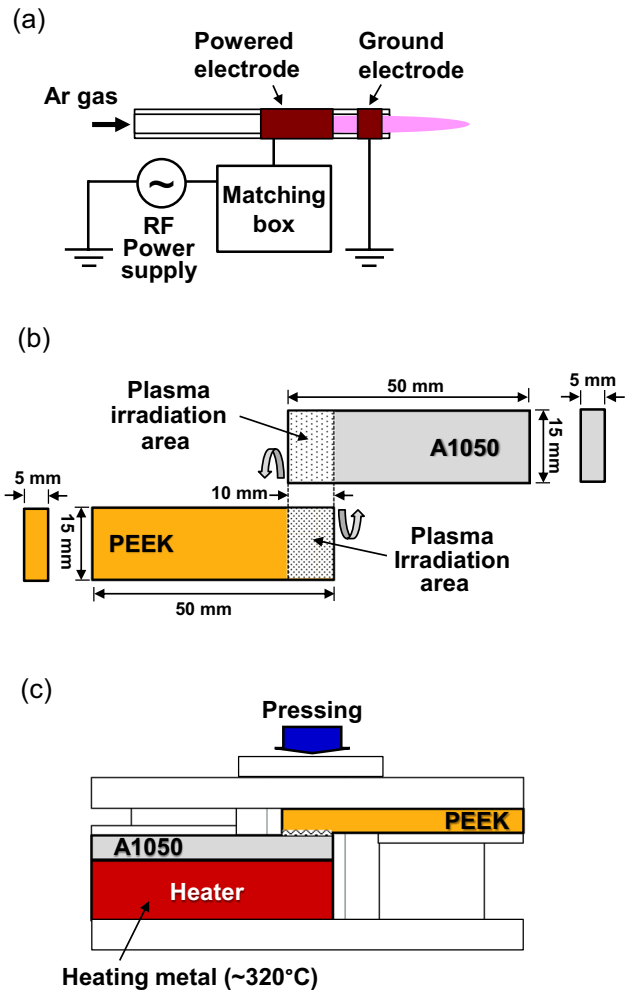

Fig. 1 Schematic illustrations of **a** an atmospheric pressure RF plasma jet, **b** the dimensions of the specimen, and **c** the configuration of A1050 and PEEK direct joining with hot-pressing process via pre-plasma treatment

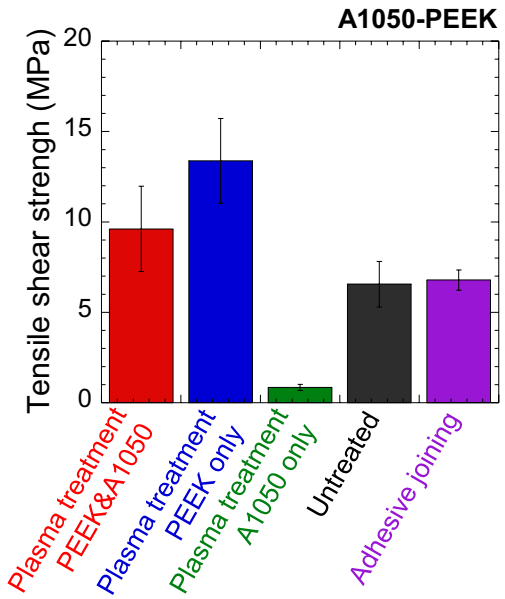

Fig. 2 Tensile shear strength of samples bonded by the hot-pressing process using an atmospheric-pressure RF plasma jet together with that of the thermocompression method using untreated A1050 and PEEK

AGS-X: Simatzu Corporation). A tensile shear strength was determined from the jointed area of bonded specimens and the maximum load at failure for the specimens measured at a crosshead speed of 1.66×10^{-3} mm/s. The bond strength of the bonded specimens was evaluated by averaging three samples.

The surface morphology analysis of A1050 sheet were carried out by scanning electron microscopy (SEM; Hitachi SU-70) and atomic force spectroscopy (AFM) (KEYENCE VN-8000). The elemental composition of A1050 surface was analyzed using the SEM with energy dispersive X-ray spectroscopy (EDX, OXFORD Instruments INCA PentaFETx3). The chemical bonding state of the plasma exposed surface was analyzed by X-ray photoelectron spectroscopy (XPS; Shimazu, AXIS165).

3 Results and discussion

The feasibility of A1050-PEEK direct joining with hot-pressing process via pre-treatment using non-thermal atmospheric pressure plasma jet has been studied.

In order to investigate the influence of plasma treatment to A1050 and PEEK surfaces on the A1050-PEEK bonding, the A1050-PEEK direct joining with hot-pressing process via pre- plasma treatment was demonstrated. Figure 2 shows the tensile shear strength of A1050-PEEK jointing samples using plasma treated only on A1050, only on PEEK, and on both A1050 and PEEK together with that of the conventional hot-pressing and adhesive. In the conventional hot-pressing and the bonding with adhesive, the tensile shear strength of was 6.6 MPa for conventional thermocompression bonding and 6.8 MPa for the bonding with adhesive, respectively. The bond strength of the sample bonded by plasma irradiated only to PEEK was 13.4 MPa, which was about 2 times as high as the bonding strength of the untreated sample. In contrast, the sample bonded of plasma-irradiated only to A1050 showed a considerable decrease in the bond strength to 0.9 MPa. Moreover, the bonding sample irradiated to both A1050 and PEEK had a bond strength of 9.6 MPa. This result indicates that the plasma irradiation of PEEK has a significant effect on bond strength in A1050-PEEK bonding. Figure 3 shows a photograph of the fractured surface after tensile testing of a specimen bonded with and without plasma irradiation. In the specimen irradiated with plasma on PEEK, it shows interfacial delamination and

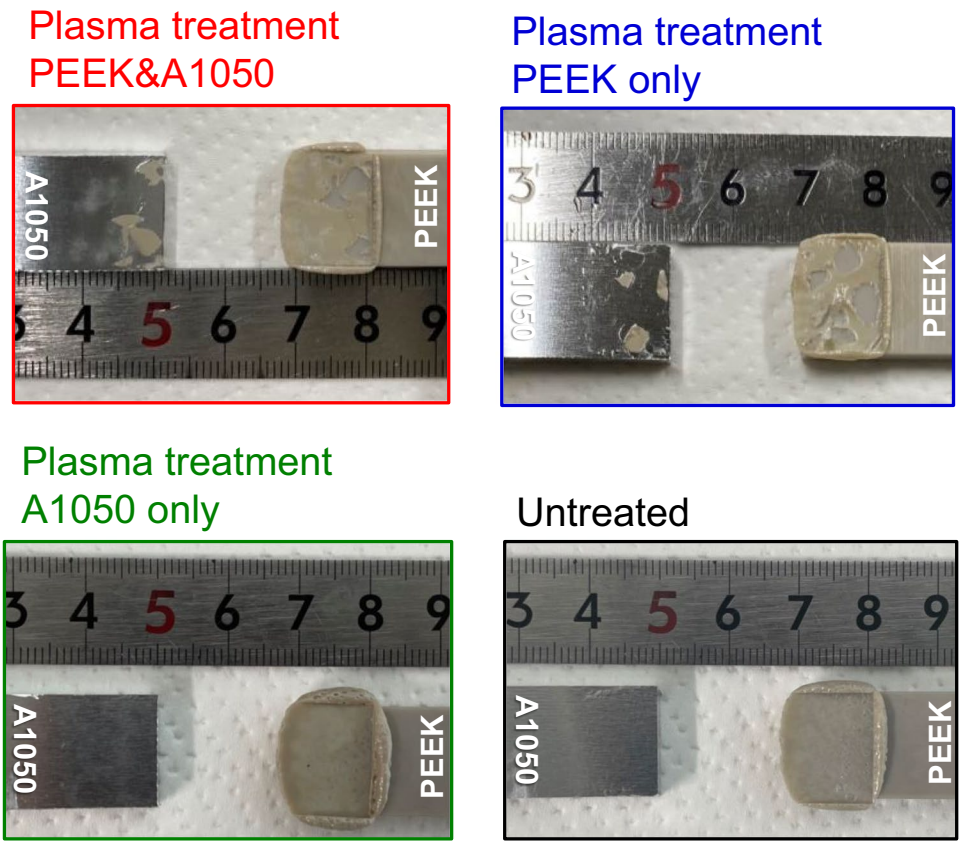

Fig. 3 Images of fracture surface after tensile testing of a specimen bonded with and without plasma irradiation

some cohesive failure with or without plasma on the A1050 side. In contrast, the specimen bonded with plasma irradiation on only A1050 side showed complete delamination. In the specimen bonded using untreated A1050 / PEEK, some cohesive delamination and interfacial delamination can be observed. In direct bonding using hot-pressing, it has already been reported that heat-induced defects occur on the PEEK side near the bonding interface when the process temperature is over 400 °C using PEEK [28], but direct bonding is performed at a lower temperature of 320 °C in the present process, so the generation of heat-induced defects is considered to be suppressed. The results show that plasma treatment on PEEK is superior to untreated PEEK in improving bond strength. On the other hand, the plasma irradiated A1050 shows a decrease in bonding strength compared to the untreated sample.

In dissimilar material direct joining, the physical and chemical state on the metal and polymer surface plays an important role with respect to bond strength. The physical effect of plasma irradiation on the A1050 surface was examined. The morphology of the A1050 surface due to plasma irradiation was observed by using AFM together with that of untreated samples. Figure 4 shows the surface roughness (R_a) estimated from results observed by AFM images of A1050 surface when the time of plasma irradiation is varied. With increasing time of plasma irradiation, the R_a of

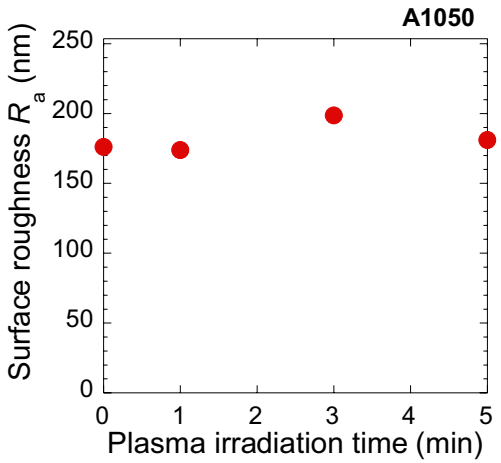

Fig. 4 Variation of surface roughness R_a of A1050 on plasma irradiation time

the A1050 surface is almost at 180 ~ 200 nm. In general, it is known that an increase in surface roughness leads to stronger bonding strength due to the anchor effect. Therefore, this result exhibits that that the contribution to joint strength in this experiment is largely due to chemical effects.

The changes in the chemical composition of A1050 surface with and without plasma irradiation were investigated

using SEM–EDX. Figure 5 shows the SEM images and SEM–EDX elemental maps of Al (blue), Fe (green), and O (red) on the A1050 surface of (a) untreated and (b) plasma irradiation for 5 min. No change in surface morphology of A1050 due to plasma irradiation was observed as shown in the SEM images in Fig. 5. Lines 2 – 4 of Fig. 5 show SEM–EDX elemental maps of Al, Fe, and O on a typical A1050 sample surface. The SEM–EDX mapping on A1050 surface showed that Al was mostly distributed on the surface, with trace amounts of Fe adhering to the surface. The O of SEM–EDX mapping shows slight Al surface oxidation. Figure 6 shows the atomic concentration of A1050 sample surface evaluated by the SEM–EDX mapping of Al, Fe, and O as a parameter of plasma irradiation time.

With increasing plasma irradiation time, the concentration of O on A1050 surface increased slightly after 1 min and then became almost constant. It is well known that the amorphous native aluminum oxide film is formed spontaneously at ambient pressures and at low temperatures and it

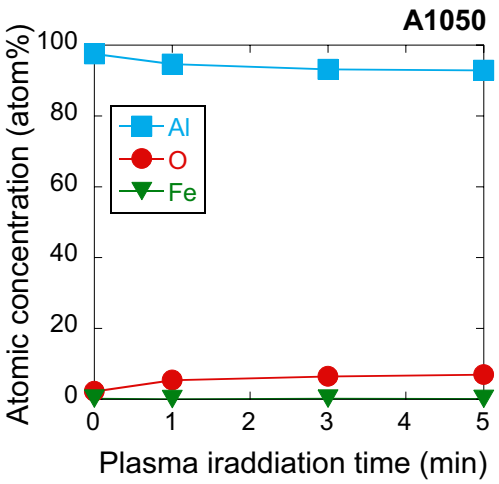

Fig. 6 Atomic concentration of A1050 sample surface evaluated by SEM–EDX mapping of Al, Fe, and O as a parameter of plasma irradiation time

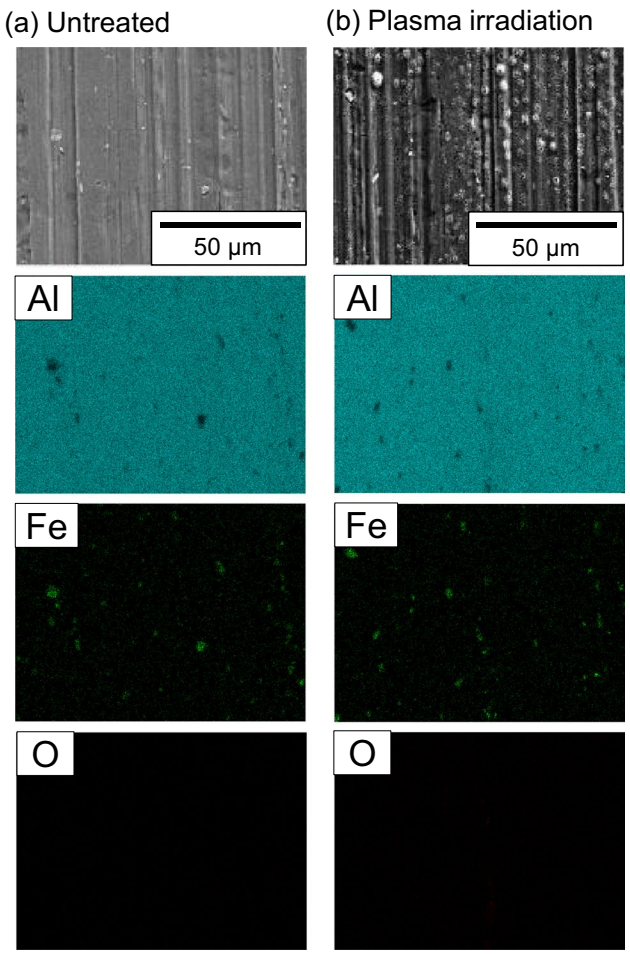

Fig. 5 SEM images and SEM–EDX elemental maps of Al (blue), Fe (green) and O (red) on the A1050 surface of **a** untreated and **b** plasma irradiation for 5 min

acts as a passive film. The formation of the passive film on aluminum is also limited by surface temperature and oxidation conditions [38, 39]. In this case, plasma irradiation accelerates oxidation immediately after irradiation due to the temperature increase caused by heat input from the plasma and the irradiation of high-density oxygen-based active species generated by a plasma jet, but the oxide growth stops and a limiting thickness is reached because the irradiation conditions stabilize. These SEM–EDX results show that the oxidation state of the surface was slightly accelerated but not significantly changed by plasma irradiation.

In order to obtain information on the chemical state of the nano surface of A1050, the chemical bonding state of A1050 surface with and without plasma irradiation was analyzed by XPS. Figure 7 shows the variation in XPS Al 2p and O 1 s spectra of A1050 surface when plasma irradiation time is varied. The Al 2p spectra were deconvoluted into the following components: Al(metal) bond at 71.3 eV, AlO_x bond at 72.3 eV, and Al_2O_3 bond at 74.1 eV [40]. The O 1 s spectra were deconvoluted into the following components: alumina (Al_2O_3) induced oxides bond at 527.7 eV and hydroxides bond at 530.0 eV [41]. The XPS Al 2p spectra of untreated surface of A1050 show the bond peak attributed to Al_2O_3 and metallic aluminum, and the XPS O 1 s spectra show peaks attributed to the naturally oxidized Al surface. On the other hand, the XPS Al 2p spectra after plasma irradiation show an increase of AlO_x bond peak on the A1050 surface, and the XPS O 1 s spectra show the considerable increase in the peaks of hydroxide (OH–) on the surface.

As shown in the XPS results, the initial surface of the A1050 is covered with Al_2O_3 formed as a natural oxide film, but a hydrated oxide layer is formed due to the injection of reactive oxygen species including oxygen

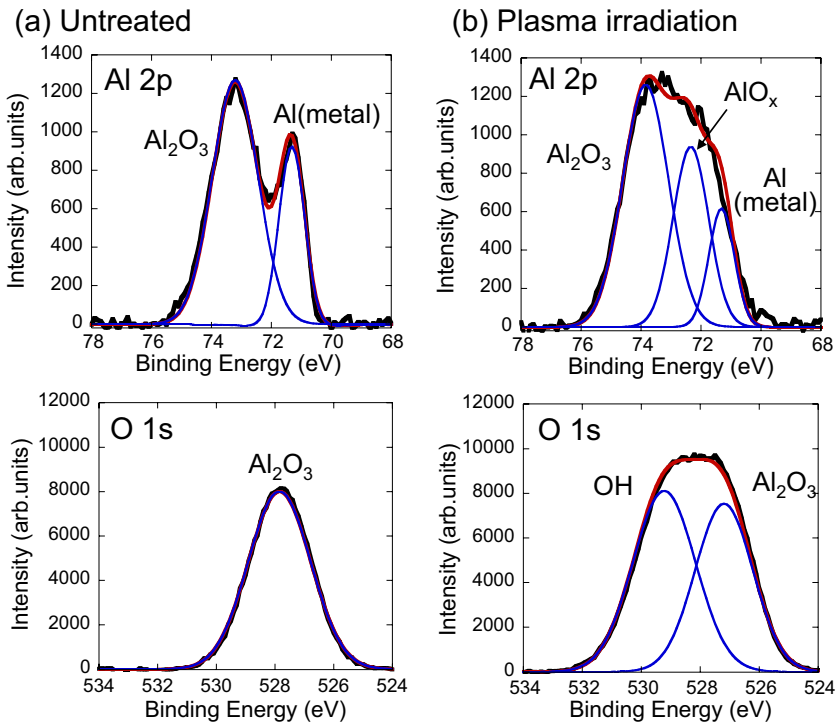

Fig. 7 Change in XPS Al2p and O1s spectra of A1050 surface with and without plasma irradiation

and hydroxyl radials, and then Al_2O_3 and hydroxide film will be mixed on the A1050 surface. This hydrated oxide layer of A1050 has an undesirable effect on bonding. In general, aluminum hydroxide formed by condensation on the surface of A1050 has low cohesion as a thin film and tends to be a weakly bonded layer [42]. These results suggest that the formation of aluminum hydroxide induced by the incident of reactive oxygen species from the plasma on A1050 reduced the bond strength between A1050 and PEEK.

The plasma irradiation effect on the PEEK surface in A1050-PEEK direct bonding was investigated. Figure 8 shows the change in tensile shear strength of A1050-PEEK samples with PEEK with varying plasma irradiation time. A1050 was used an untreated sample. With increasing the plasma irradiation time, the tensile shear strength of the A1050-PEEK samples increased moderately from 6.6 MPa for 0 min to 13.4 MPa for 5 min and then was almost constant. In previous study, the chemical bonding state of plasma-irradiated PEEK surface have been investigated by using XPS [43]. The XPS observation of chemical bonding state shows that O–C = O bonds, which were not present in the chemical structure of as-received PEEK, are formed by plasma irradiation in addition to the C = O and C–O bonds derived from the chemical structure of PEEK. With increasing the plasma irradiation time, the peak intensity of these bonds on the PEEK surface was increased. In direct metal-polymer dissimilar material bonding, it is generally known that

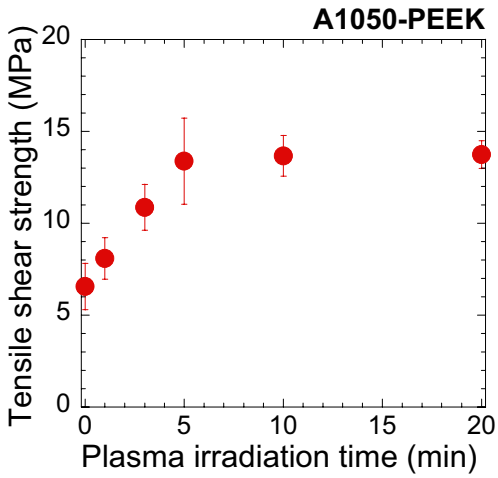

Fig. 8 Variation of tensile shear strength of A1050-PEEK bonded samples in a case of PEEK only were irradiated with plasma as a function of plasma irradiation time

O = C–O bonding on the polymer surface contributes to the bond strength between the materials [44–46]. These results exhibit the irradiation of oxidation contributing radicals generated by the plasma jet contributes to the addition of oxygen functional groups on the surface of the PEEK. Therefore, efficient oxidation of the surface of the PEEK using atmospheric pressure RF plasma jet is effective in increasing bond strength in A1050-PEEK direct joining.

One of the pre-treatment methods for direct metal-polymer bonding is laser texturing, which is expected to enhance bonding strength by creating a physical surface structure. In laser texturing, a texture is created on the metal side with a laser in advance to allow the polymer to fully penetrate into the structure, resulting in sufficiently high bond strength [28–30]. However, since the metal must be heated sufficiently above the melting point of the polymer (for example; ~ 400 °C for PEEK), damage to the polymer at the interface is a concern. On the other hand, surface treatment by plasma irradiation increases the chemical bonding point of both metal and polymer at the time of bonding by adding functional groups to the metal and polymer, enabling bonding at a temperature near the melting point and making strong bonding possible.

For these reasons, these results show that pre-treatment with non-thermal atmospheric pressure plasma jet in A1050-PEEK direct joining using hot-press is an effective means of improving bond strength.

4 Conclusions

A1050-PEEK direct joining with hot-pressing process via pre-treatment using non-thermal atmospheric pressure plasma jet has been performed. The effect of plasma irradiation on strength of A1050-PEEK direct joining was investigated. The tensile shear strength of A1050-PEEK bonded samples, bonded by a combination of hot-pressing process and pre-plasma treatment using non-thermal atmospheric pressure plasma jet, has been compared with that of conventional hot-pressing and adhesive bonded samples made of A1050 and PEEK.

(1) A1050-PEEK bonded samples with plasma-treated PEEK only showed high tensile shear stress of 13.4 MPa. This increase in tensile shear strength is considered to be attributed to the addition of oxygen functional groups on the surface of the PEEK by reactive oxygen species generated by the plasma jet.
(2) On the other hand, the tensile shear strength of plasma-irradiated A1050 bonding samples was lower than that of unirradiated samples. The decrease in bond strength due to plasma irradiation of A1050 is considered to be caused by aluminum hydroxide formed by condensation on the surface of A1050 during plasma irradiation since this hydrated oxide layer of A1050 has low cohesion as a thin film and tends to be a weakly bonded layer.
(3) The plasma irradiation effect on the PEEK surface in A1050-PEEK direct bonding was investigated in the case of which A1050 was used an untreated sample. With increasing the plasma irradiation time, the tensile shear strength of the A1050-PEEK samples increased moderately from 6.6 MPa for 0 min to 13.4 MPa for 5 min and then was almost constant. With increasing the plasma irradiation time, the peak intensity of these bonds on the PEEK surface was increased. These results exhibit the irradiation of oxidation contributing radicals generated by the plasma jet contributes to the addition of oxygen functional groups on the surface of the PEEK.

Author contribution KT contributed to all parts of this work: conceptualization, investigation, and writing the manuscript. AJ, SN, RK, and ST contributed to collecting and analyzing the data of surface measurement and the joining experiments. GU contributed to assistance of conceptualization and analyzing the data of investigation. YS contributed to conceptualization, supervision, and project administration. All authors read and approved the final manuscript.

Funding Open access funding provided by Osaka University.

Declarations

Ethics approval Not applicable.

Consent to participate Not applicable.

Consent for publication The authors give the publisher the consent to publish the work.

Competing interests The authors declare no competing interests.

References

1. Sakundarini N, Taha Z, Abdul-Rashid SH, Ghazila RAR (2013) Optimal multi-material selection for lightweight design of automotive body assembly incorporating recyclability. Mater Des 50:846–857. https://doi.org/10.1016/j.matdes.2013.03.085
2. Braga DFO, Tavares SMO, da Silva LFM, Moreira PMGP, de Castro PMST (2014) Advanced design for lightweight structures: review and prospects. Prog Aerosp Sci 69:29–39. https://doi.org/10.1016/j.paerosci.2014.03.003

3. Quazi MM, Ishak M, Fazal MA, Arslan A, Rubaiee S, Aiman MH, Qaban A, Yusof F, Sultan T, Ali MM, Manladan SM (2021) A comprehensive assessment of laser welding of biomedical devices and implant materials: recent research, development and applications. Crit Rev Solid State Mater Sci 46:109–151. https://doi.org/10.1080/10408436.2019.1708701
4. Bakar WZW, Basri S, Jamaludin SNS, Sajjad A (2018) Functionally graded materials: an overview of dental applications. World J Dent 9:137–144. https://doi.org/10.5005/jp-journals-10015-1523
5. Lambiase F, Scipioni SI, Lee C-J, Ko D-C, Liu F (2021) A state-of-the-art review on advanced joining processes for metal-composite and metal-polymer hybrid structures. Materials 14:1890. https://doi.org/10.3390/ma14081890
6. Nicoletti L, Romano A, König A, Köhler P, Heinrich M, Lienkamp M (2021) An estimation of the lightweight potential of battery electric vehicles. Energies (Basel) 14:4655. https://doi.org/10.3390/en14154655
7. Zhao H, Zhang R, Bin Z (2018) A review of automotive lightweight technology. Adv Eng Res 149:31–34. https://doi.org/10.2991/MECAE-18.2018.10
8. Tong L (1998) Failure of adhesive-bonded composite single lap joints with embedded cracks. AIAA J 36:448–456. https://doi.org/10.2514/2.385
9. Cheuk PT, Tong L (2002) Failure of adhesive bonded composite lap shear joints with embedded precrack. Compos Sci Technol 62:1079–1095. https://doi.org/10.1016/S0266-3538(02)00054-4
10. Marannano G, Zuccarello B (2015) Numerical experimental analysis of hybrid double lap aluminum-CFRP joints. Compos B Eng 71:28–39. https://doi.org/10.1016/j.compositesb.2014.11.025
11. Amancio-Filho ST, Dos Santos JF (2009) Joining of polymers and polymer-metal hybrid structures: recent developments and trends. Polym Eng Sci 49:1461–1476. https://doi.org/10.1002/pen.21424
12. Martinsen K, Hu SJ, Carlson BE (2015) Joining of dissimilar materials. CIRP Ann 64:679–699. https://doi.org/10.1016/J.CIRP.2015.05.006
13. Zhou Z, Gao X, Zhang Y (2022) Research progress on characterization and regulation of forming quality in laser joining of metal and polymer, and development trends of lightweight automotive applications. Metals (Basel) 12:1666. https://doi.org/10.3390/met12101666
14. Feistauer EE, dos Santos JF, Amancio-Filho ST (2019) A review on direct assembly of through-the-thickness reinforced metal–polymer composite hybrid structures. Polym Eng Sci 59:661–674. https://doi.org/10.1002/pen.25022
15. Vasconcelos RL, Oliveira GHM, Amancio-Filho ST, Canto LB (2023) Injection overmolding of polymer-metal hybrid structures: a review. Polym Eng Sci 63:691–722. https://doi.org/10.1002/pen.26244
16. Balle F, Wagner G, Eifler D (2007) Ultrasonic spot welding of aluminum sheet/carbon fiber reinforced polymer—joints. Materwiss Werksttech 38:934–938. https://doi.org/10.1002/mawe.200700212
17. Balle F, Wagner G, Eifler D (2009) Ultrasonic metal welding of aluminium sheets to carbon fibre reinforced thermoplastic composites. Adv Eng Mater 11:35–39. https://doi.org/10.1002/adem.200800271
18. Balle F, Eifler D (2012) Statistical test planning for ultrasonic welding of dissimilar materials using the example of aluminum-carbon fiber reinforced polymers (CFRP) joints. Materwiss Werksttech 43:286–292. https://doi.org/10.1002/mawe.201200943
19. Mitschang P, Velthuis R, Didi M (2013) Induction spot welding of metal/CFRPC hybrid joints. Adv Eng Mater 15:804–813. https://doi.org/10.1002/adem.201200273
20. Katayama S, Kawahito Y (2008) Laser direct joining of metal and plastic. Scr Mater 59:1247–1250. https://doi.org/10.1016/j.scriptamat.2008.08.026
21. Lamberti C, Solchenbach T, Plapper P, Possart W (2014) Laser assisted joining of hybrid polyamide-aluminum structures. Phys Procedia 56:845–853. https://doi.org/10.1016/j.phpro.2014.08.103
22. Jung KW, Kawahito Y, Takahashi M, Katayama S (2013) Laser direct joining of carbon fiber reinforced plastic to zinc-coated steel. Mater Des 47:179–188. https://doi.org/10.1016/j.matdes.2012.12.015
23. Davies RJ, Kinloch AJ (1989) The surface characterisation and adhesive bonding of aluminium. Adhesion 13:8–22. https://doi.org/10.1007/978-94-010-9082-7_2
24. Liu FC, Liao J, Nakata K (2014) Joining of metal to plastic using friction lap welding. Mater Des 54:236–244. https://doi.org/10.1016/j.matdes.2013.08.056
25. Hakamada M, Kohashi Y, Yamano Y, Mabuchi M (2018) Joining of anodized and stacked aluminum sheets by copper electrodeposition: nano-anchor effect. Mater Trans 59:324–326. https://doi.org/10.2320/matertrans.M2017315
26. Faulkner KDB, Harcourt JK (1975) Silane coupling agents in stainless steel and polymethyl methacrylate systems. Aust Dent J 20:86–88. https://doi.org/10.1111/j.1834-7819.1975.tb04334.x
27. Kotha SP, Lieberman M, Vickers A, Schmid SR, Mason JJ (2006) Adhesion enhancement of steel fibers to acrylic bone cement through a silane coupling agent. J Biomed Mater Res A 76A:111–119. https://doi.org/10.1002/jbm.a.30543
28. Lambiase F, Genna S (2018) Experimental analysis of laser assisted joining of Al-Mg aluminium alloy with polyetheretherketone (PEEK). Int J Adhes Adhes 84:265–274. https://doi.org/10.1016/j.ijadhadh.2018.04.004
29. Lambiase F, Genna S (2018) Laser assisted joining of AA5053 aluminum alloy with polyvinyl chloride (PVC). Opt Laser Technol 107:80–88. https://doi.org/10.1016/j.optlastec.2018.05.023
30. Rodríguez-Vidal E, Sanz C, Lambarri J, Quintana I (2018) Experimental investigation into metal micro-patterning by laser on polymer-metal hybrid joining. Opt Laser Technol 104:73–82. https://doi.org/10.1016/j.optlastec.2018.02.003
31. Ha SW, Hauert R, Ernst KH, Wintermantel E (1997) Surface analysis of chemically-etched and plasma-treated polyetheretherketone (PEEK) for biomedical applications. Surf Coat Technol 96:293–299. https://doi.org/10.1016/S0257-8972(97)00179-5
32. Shi H, Sinke J, Benedictus R (2017) Surface modification of PEEK by UV irradiation for direct co-curing with carbon fibre reinforced epoxy prepregs. Int J Adhes Adhes 73:51–57. https://doi.org/10.1016/j.ijadhadh.2016.07.017
33. Comyn J, Mascia L, Xiao G, Parker BM (1996) Corona-discharge treatment of polyetheretherketone (PEEK) for adhesive bonding. Int J Adhes Adhes 16:301–304. https://doi.org/10.1016/S0143-7496(96)00010-3
34. Endo T, Reddy L, Nishikawa H, Kaneko S, Nakamura Y, Endo K (2017) Composite engineering—direct bonding of plastic PET films by plasma irradiation. Procedia Eng 171:88–103. https://doi.org/10.1016/j.proeng.2017.01.315
35. Uchida G, Kawabata K, Ito T, Takenaka K, Setsuhara Y (2017) Development of a non-equilibrium 60 MHz plasma jet with a long discharge plume. J Appl Phys 122:033301. https://doi.org/10.1063/1.4993715
36. Uchida G, Takenaka K, Takeda K, Ishikawa K, Hori M, Setsuhara Y (2018) Selective production of reactive oxygen and nitrogen species in the plasma-treated water by using a nonthermal high-frequency plasma jet. Jpn J Appl Phys 57:0102B4. https://doi.org/10.7567/JJAP.57.0102B4
37. Takenaka K, Machida R, Bono T, Jinda A, Toko S, Uchida G, Setsuhara Y (2022) Development of a non-thermal atmospheric pressure plasma-assisted technology for the direct joining of metals

with dissimilar materials. J Manuf Process 75:664–669. https://doi.org/10.1016/j.jmapro.2022.01.041
38. Cabrera N, Mott NF (1949) Theory of the oxidation of metals. Rep Prog Phys 12:163–184. https://doi.org/10.1088/0034-4885/12/1/308
39. Fehlner FP, Mott NF (1970) Low-temperature oxidation. Oxid Met 2:59–99. https://doi.org/10.1007/BF00603582
40. Hoque E, DeRose JA, Hoffmann P, Mathieu HJ, Bhushan B, Cichomski M (2006) Phosphonate self-assembled monolayers on aluminum surfaces. J Chem Phys 124:174710. https://doi.org/10.1063/1.2186311
41. Tago T, Kataoka N, Tanaka H, Kinoshita K, Kishida S (2017) XPS study from a clean surface of Al_2O_3 single crystals. Procedia Eng 216:175–181. https://doi.org/10.1016/J.PROENG.2018.02.081
42. Kudo T, Alwitt RS (1978) Cross-sections of hydrous and composite aluminum oxide films. Electrochim Acta 23:341–345. https://doi.org/10.1016/0013-4686(78)80072-3
43. Takenaka K, Jinda A, Nakamoto S, Toko S, Uchida G, Setsuhara Y (2023) Direct bonding of stainless steel and PEEK using non-thermal atmospheric pressure plasma-assisted joining technology. J Manuf Process 105:276–281. https://doi.org/10.1016/j.jmapro.2023.09.049
44. Ochoa-Putman C, Vaidya UK (2011) Mechanisms of interfacial adhesion in metal-polymer composites—effect of chemical treatment. Compos Part A Appl Sci Manuf 42:906–915. https://doi.org/10.1016/j.compositesa.2011.03.019
45. Comyn J, Mascia L, Xiao G, Parker BM (1996) Plasma-treatment of polyetheretherketone (PEEK) for adhesive bonding. Int J Adhes Adhes 16:97–104. https://doi.org/10.1016/0143-7496(96)89798-3
46. Laurens P, Sadras B, Decobert F, Arefi-Khonsari F, Amouroux J (1998) Enhancement of the adhesive bonding properties of PEEK by excimer laser treatment. Int J Adhes Adhes 18:19–27. https://doi.org/10.1016/S0143-7496(97)00063-8